

# Open-Shell Organometallic $[M^{\text{II}}(\text{dbcot}(\text{bislutidylamine}))]^{2+}$ Complexes ( $M = \text{Rh}, \text{Ir}$ ): Unexpected Base-Assisted Reduction of the Metal Instead of Amine Ligand Deprotonation

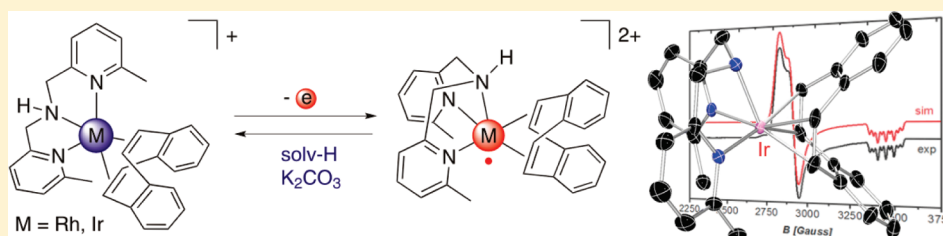
Wojciech I. Dzik,<sup>†</sup> Luis Fuente Arruga,<sup>†</sup> Maxime A. Siegler,<sup>‡</sup> Anthony L. Spek,<sup>‡</sup> Joost N. H. Reek,<sup>†</sup> and Bas de Bruin<sup>\*,†</sup>

<sup>†</sup>Van 't Hoff Institute for Molecular Sciences, University of Amsterdam, Science Park 904, 1098 XH Amsterdam, The Netherlands

<sup>‡</sup>Bijvoet Center for Biomolecular Research, Utrecht University, Utrecht, The Netherlands

**S** Supporting Information

## ABSTRACT:



Cationic rhodium and iridium complexes with dibenzo[*a,e*]cyclooctatetraene (dbcot) and bislutidylamine (bla) were synthesized from the respective  $[M(\mu\text{-Cl})(\text{dbcot})]_2$  dimers and the bla ligand and were characterized by NMR, X-ray diffraction, and cyclic voltammetry. Both  $[M^{\text{I}}(\text{dbcot})(\text{bla})]^+$  complexes are easily oxidized by one electron to form paramagnetic dicationic analogues  $[M^{\text{II}}(\text{dbcot})(\text{bla})]^{2+}$  ( $M = \text{Rh}, \text{Ir}$ ). In the solid state, the geometry changes from a distorted trigonal bipyramid to square pyramidal upon oxidation of the metal from  $M^{\text{I}}$  to  $M^{\text{II}}$ , as evidenced by X-ray diffraction studies of the iridium complexes. The paramagnetic complexes undergo facile one-electron reduction in the presence of base, most likely involving oxidation of the solvent or hydroxide anions. A control experiment using the corresponding  $[\text{Rh}^{\text{II}}(\text{dbcot})(\text{Bn-bla})]^{2+}$  complex, wherein Bn-bla is the *N*-benzyl-protected bla ligand, gives similar results, which strongly suggests that deprotonation of the N–H moiety of the  $[M^{\text{II}}(\text{dbcot})(\text{bla})]^{2+}$  plays a minor role (if any at all) in the observed base-mediated reduction processes. Reaction of bla with  $[\text{Ir}(\mu\text{-Cl})(\text{coe})]_2$  (coe = *cis*-cyclooctene) results in oxidative addition of the vinylic C–H bond of coe to the metal center, as evidenced by X-ray diffraction.

## INTRODUCTION

Hydrogen atom transfer (HAT) plays an important role in inorganic chemistry and is of fundamental importance in many biochemical transformations and some industrially relevant synthetic reactions. Transfer of a hydrogen atom from the substrate to a metal-coordinated oxygen atom is one of the key steps in biotransformations catalyzed by galactose oxidase,<sup>1</sup> lipoxygenase,<sup>2</sup> cytochrome P<sub>450</sub>,<sup>3</sup> methane monooxygenases,<sup>4</sup> and class I ribonucleotide reductase.<sup>5</sup> HAT reactions are essential for chain transfer during metal-mediated radical polymerization of olefins,<sup>6</sup> but can also lead to catalyst deactivation in cyclopropanation reactions.<sup>7</sup>

Open-shell second- and third-row transition metal complexes are excellent models to study HAT reactions, because the products are generally well-defined NMR-characterizable diamagnetic compounds. This has been exploited by a number of groups over the past years, providing information on the fundamental reactivity of transition metal radical complexes toward Y–H bonds ( $Y = \text{C}, \text{H}, \text{Si}, \text{S}$ ). The pioneering work of the group of Wayland on rhodium and iridium complexes has

demonstrated that C–H<sup>8</sup> and H–H<sup>8c</sup> bonds can be broken homolytically between two metalloradicals. Ligand radicals generated on these metals are also capable of abstracting hydrogen atoms from the reaction medium.<sup>7,9</sup> Recently, the group of Grützmacher elegantly presented a galactose oxidase mimic based on an iridium aminyl radical complex.<sup>10</sup> The study of hydrogen atom transfer at open-shell second- and third-row transition metal complexes clearly deserves much more attention, as we are only beginning to understand such reactivity.

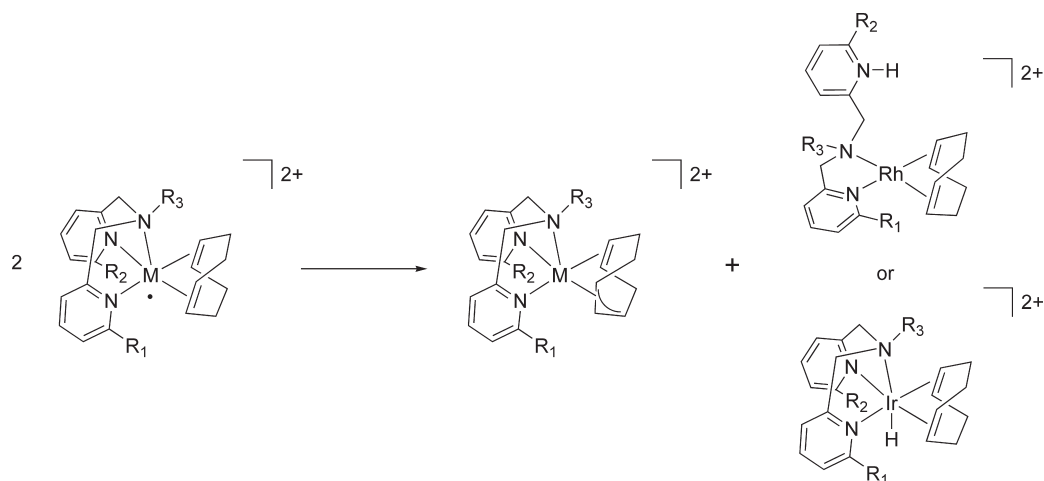
Recently, our group investigated the reactivity of paramagnetic rhodium and iridium compounds with the general formula  $[M^{\text{II}}(\text{N}_3\text{-ligand})(\text{cod})]^{2+}$  (cod = *Z,Z*-1,5-cyclooctadiene).

These complexes undergo interesting bimolecular HAT reactions, and the rate of the HAT pathway proved to be markedly dependent on the nature of the used bispicolylamine (bpa)-type N<sub>3</sub> ligand. Irrespective of the R groups introduced in the bpa moiety ( $R_1, R_2 = \text{H}$  or Me,  $R_3 = \text{H}$  or Bn) the paramagnetic

**Received:** December 8, 2010

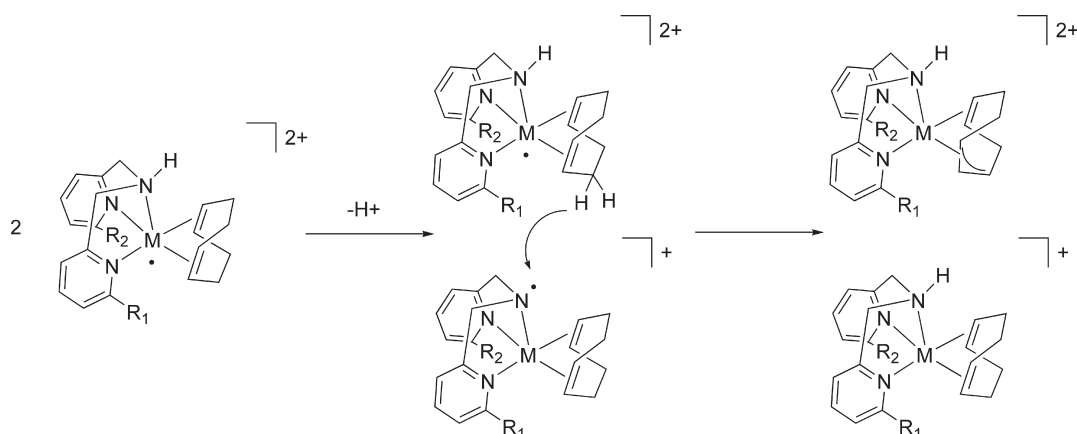
**Published:** March 10, 2011



Scheme 1. Hydrogen Atom Transfer of Allylic Hydrogen in  $[M^{II}(N_3\text{-ligand})(\text{cod})]^{2+}$  Complexes<sup>a</sup>

<sup>a</sup>  $R_1, R_2 = \text{H or Me}$ ,  $R_3 = \text{H or Bn}$ .

Scheme 2. Possible Hydrogen Atom Transfer of the Allylic Hydrogen of the Cod Ligand via a Putative Aminyl Radical Species



complexes spontaneously transform into a 1:1 mixture of  $[M^{III}(\text{allyl})(N_3\text{-ligand})]^{2+}$  and protonated  $M(\text{cod})$  complexes (in the form of  $[M^I(\text{olefin})(N_3\text{-ligand}+H)]^{2+}$  for  $M = \text{Rh}$  or  $[M^{III}(\text{H})(\text{olefin})(N_3\text{-ligand})]^{2+}$  for  $M = \text{Ir}$ , Scheme 1).<sup>11</sup> The rate of decomposition depends strongly on the nature of substituents, and only the complexes with  $R_1, R_2 = \text{Me}$ ,  $R_3 = \text{Bn}$  were stable enough to be isolated and fully characterized. The low stability of complexes with secondary amine bpa-type ligands ( $R_3 = \text{H}$ ) raises the question if the decomposition to the allyl and hydride complexes could proceed via the involvement of aminyl radicals (Scheme 2).

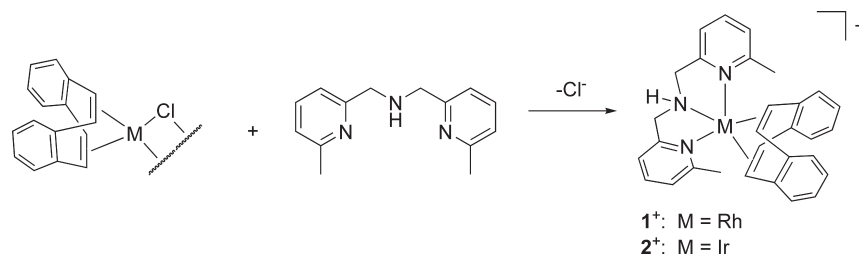
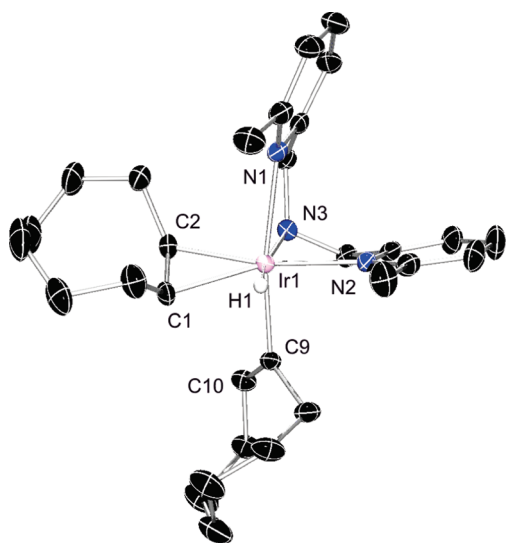
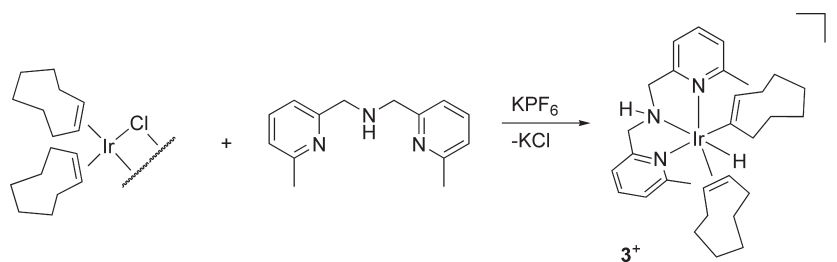
The possible involvement of aminyl radicals in the  $[M^{II}(\text{cod})(N_3\text{-ligand})]^{2+}$  system seems plausible. Aminyl radicals can be stabilized by coordination to a metal center, and several examples of such stable species have been reported.<sup>12,13</sup> Reversible H atom transfer (HAT) from a nitrogen atom of a transition metal complex with a ligand possessing an amine functionality can occur and has been extensively studied in the past decade by the group of Mayer.<sup>14</sup> Recently, Grützmacher et al. showed that amine-diolefin Rh(I) and Ir(I) complexes can form stable, d<sup>8</sup> transition metal aminyl radical complexes upon deprotonation of the amine and subsequent one-electron

oxidation.<sup>10,15</sup> These aminyl radical complexes abstract hydrogen atoms from activated Y–H bonds. Moreover, bispicolylamine (bpa) is also prone to mono- and double-deprotonation when coordinated to rhodium or iridium diolefin species<sup>16</sup> and can subsequently form transient ligand<sup>16a,c,d</sup>-centered radical species upon one-electron oxidation.

To study the possible aminyl radical reactivity of the bpa-type ligand, we need a diene ligand that is more robust than cyclooctadiene (innocent toward allylic C–H bond activation or C–C coupling). Therefore we decided to synthesize rhodium and iridium complexes with dibenzo[*a,e*]cyclooctatetraene (dbcot) as the supporting diolefin.<sup>17</sup> Since the steric shielding of the metal center proved to have a positive effect on the stability of  $[M^{II}(\text{cod})(N_3\text{-ligand})]^{2+}$  complexes, we chose bislutidylamine (bla) as the  $N_3$ -donor ligand.

## RESULTS AND DISCUSSION

**Synthesis and Characterization of  $[M^I(\text{bla})(\text{dbcot})]^+$  Complexes.** Complexes  $[\text{Rh}(\eta^4\text{-dbcot})(\kappa^3\text{-bla})]\text{PF}_6$  (**[1]** $\text{PF}_6$ ) and  $[\text{Ir}(\eta^4\text{-dbcot})(\kappa^3\text{-bla})]\text{PF}_6$  (**[2]** $\text{PF}_6$ ) (dbcot = dibenzo[*a*,

Scheme 3. Synthesis of  $[\text{Rh}(\eta^4\text{-dbcot})(\kappa^3\text{-bla})]^+$  ( $1^+$ ) and  $[\text{Ir}(\eta^4\text{-dbcot})(\kappa^3\text{-bla})]^+$  ( $2^+$ )Scheme 4. Synthesis of  $[\text{Ir}(\kappa^3\text{-bla})(\text{H})(\sigma\text{-C}_8\text{H}_{13})(\eta^2\text{-C}_8\text{H}_{14})]^+$  ( $3^+$ )

**Figure 1.** X-ray structure of  $[\text{Ir}(\text{H})(\sigma\text{-C}_8\text{H}_{13})(\eta^2\text{-C}_8\text{H}_{14})(\kappa^3\text{-bla})]^+$  ( $3^+$ ). Displacement ellipsoids are drawn at the 50% probability level (hydrogen atoms and the  $\text{PF}_6^-$  counterion were omitted for clarity). Selected bond distances (Å) and angles (deg): Ir–N1 2.239(3); Ir–N2 2.136(2); Ir–N3 2.174(3); Ir–C1 2.200(3); Ir–C2 2.168(3); Ir–C9 2.041(3); Ir–H1 1.490(3); C1–C2 1.387(5); C9–C10 1.326(4); N1–Ir–N3 79.31(10); N1–Ir–N2 82.12(10); N2–Ir–N3 78.12(9); C1–Ir–C2 37.02(12); Ir–C9–C10 123.04(2); N1–Ir1–C9 167.63(11); N2–Ir1–C9 88.13(11); N3–Ir1–C9 91.29(11); N3–Ir1–H1 170.0(11); N2–Ir1–H1 92.2(11); N1–Ir1–H1 97.0(11); H1–Ir1–C9 91.0(11).

$e$ ]cyclooctatetraene, bla = bis-*N,N*-(6-methyl-2-pyridylmethyl)-amine) were synthesized from the bla ligand and the corresponding dinuclear  $[\text{M}(\mu\text{-Cl})(\eta^4\text{-dbcot})]_2$  compounds in methanol followed by precipitation as a  $\text{PF}_6^-$  salt by adding  $\text{KPF}_6$  (Scheme 3).

$[\text{Rh}(\mu\text{-Cl})(\eta^4\text{-dbcot})]_2$  used for the synthesis of  $1^+$  could be generated *in situ* from  $[\text{Rh}(\mu\text{-Cl})(\eta^2\text{-coe})_2]_2$  (coe = *cis*-cyclooctene) and dbcot by exchange of the coe ligands bound to rhodium for dbcot. A similar approach to synthesize the iridium complex  $2^+$  failed and resulted in unexpected formation of a new complex,  $[\text{Ir}(\kappa^3\text{-bla})(\text{H})(\sigma\text{-C}_8\text{H}_{13})(\eta^2\text{-C}_8\text{H}_{14})]\text{PF}_6$  ( $[3]\text{PF}_6$ ), by oxidative addition of a vinylic C–H bond of coe to the iridium metal center (Scheme 4). Therefore the successful synthesis of  $[2]\text{PF}_6$  required the use of the isolated  $[\text{M}(\mu\text{-Cl})(\eta^4\text{-dbcot})]_2$ .

Oxidative addition of the vinylic C–H bond of cyclooctene was previously reported for iridium complexes with  $\text{HB}(\text{Pz})_3$ <sup>18</sup> and  $\text{Cn}^{19}$   $\text{N}_3$ -supporting ligands ( $\text{HB}(\text{Pz})_3$  = tris(pyrazolyl)borate,  $\text{Cn}$  = 1,4,7-triazacyclononane). Such reactivity is in line with comparable electronic properties of tris(pyrazolyl)borate- and bislutidyl-amine-type ligands, which resulted in similar reactivity of the iridium biscarbonyl complexes toward nucleophiles.<sup>20</sup> Other electron-rich (PNP) tridentate ligands also allow for such reactivity on the iridium center.<sup>21</sup> X-ray quality crystals of  $[3]\text{PF}_6$  were grown by layering an acetone solution of  $[3]\text{PF}_6$  with hexanes (Figure 1). The structure of  $3^+$  is noteworthy and is an interesting example of a metal-olefin-hydride complex that does not undergo spontaneous olefin insertion into the M–H bond in coordinating solvents (e.g., acetone).  $[\text{Ir}(\kappa^3\text{-bla})(\text{H})(\sigma\text{-C}_8\text{H}_{13})(\eta^2\text{-C}_8\text{H}_{14})]\text{PF}_6$  has a distorted octahedral geometry with the bla ligand being coordinated in a *fac*-mode. The most sterically hindered position *trans* to the N3 amine nitrogen is occupied by the least sterically demanding hydride anion. The cyclooctenyl group coordinates *trans* to the N1 lutidyl nitrogen, and its C9–C10 bond has a clear double-bond character (1.326(4) Å). This vinylic double bond has no significant interaction with the metal. The cyclooctenyl group has a large *trans* influence on the lutidyl N1 atom, which results in a rather large (>2.23 Å) Ir–N1 distance. The cyclooctene ligand coordinates *trans* to the N2 lutidyl nitrogen. As expected for an olefin coordinated to an electron-deficient metal, the double

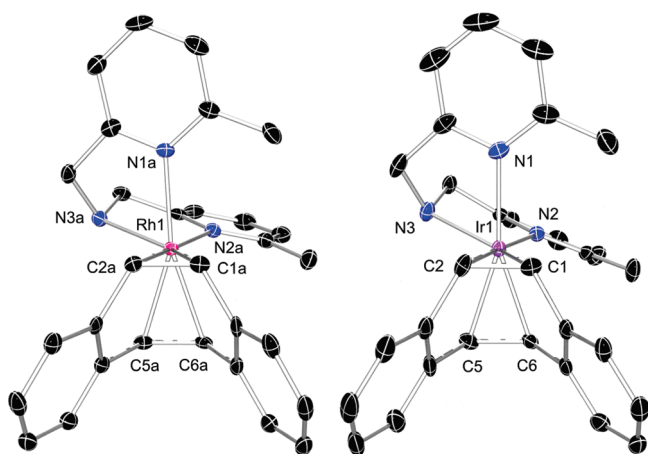


**Figure 2.** X-ray structure of  $[\text{Rh}(\eta^4\text{-dbcot})(\kappa^3\text{-bla})]^+$  ( $1^+$ ) (left) and  $[\text{Ir}(\eta^4\text{-dbcot})(\kappa^3\text{-bla})]^+$  ( $2^+$ ) (right). Displacement ellipsoids are drawn at the 50% probability level (hydrogen atoms, the  $\text{PF}_6^-$  counterions, and solvent molecules are omitted for clarity). The crystal of  $1^+$  reveals the presence of two independent but isostructural cations in the asymmetric unit. See Table 1 for selected bond distances and angles.

bond of the cyclooctene ligand does not reveal substantial elongation.

Single crystals of  $[1]\text{PF}_6$  and  $[2]\text{PF}_6$  suitable for X-ray structure determination were grown from acetone solutions layered with hexanes or diethyl ether, respectively. The two compounds are isostructural in the solid state (Figure 2) and are best described as distorted trigonal bipyramids (*tbpy*). The axial positions of the trigonal bipyramid are occupied by the lutidyl (N1) nitrogen atom and a double bond of the dbcot ligand (C5–C6). The M–N1 distance is the same for both complexes within the experimental error, while the axially coordinated double bond binds more strongly to iridium (resulting in shorter M–C5 and M–C6 distances and longer C5–C6 distance in  $2^+$  compared to  $1^+$ ).<sup>22</sup> The equatorial sites are coordinated with lutidyl N2, amine N3, and the C1–C2 double bond of dbcot. For both complexes there is no significant difference between their M–N2 and M–N3 distances; however these nitrogen atoms are bound more strongly to iridium with on average 0.03 Å shorter M–N bonds for  $2^+$  compared to the rhodium analogue  $1^+$ . The axially coordinated lutidyl moiety (N1) is bound more strongly to the metal than the equatorially bound N2 and N3 donors, as expected for a  $d^8$  *tbpy* complex.<sup>23</sup> Due to stronger  $\pi$ -back bonding in the equatorial plane of *tbpy* complexes,<sup>23</sup> the C1–C2 double bond is bound stronger compared to the axially coordinated C5–C6 bond. The metal C1–C2 interaction has a significant metalla(III)cyclopropane character, resulting in a remarkable elongation of the C1–C2 distance (1.32, 1.44, and 1.47 Å for free dbcot,<sup>24</sup>  $1^+$  and  $2^+$ , respectively). This substantial elongation of the double bonds of coordinated dbcot is indicative of strong  $\pi$ -acidity of this ligand.

In solution  $1^+$  is fluxional on the NMR time scale, leading to averaged  $^1\text{H}$  and  $^{13}\text{C}$  NMR signals for both lutidyl groups of the bla ligand and averaged signals of the two olefinic HC=CH moieties and the aromatic rings of the dbcot ligand. Analogous behavior was observed for  $2^+$ . Strong  $\pi$ -back-bonding from the metal to the dbcot ligand results in substantial upfield shifts of both the proton and carbon resonance frequencies (6.78, 4.50, and 4.37 ppm in  $^1\text{H}$  and 133.2, 74.6, and 58.3 ppm in  $^{13}\text{C}$  for free dbcot,  $1^+$ , and  $2^+$ , respectively). Thus, both the X-ray and NMR analyses confirm a very strong  $\pi$ -bonding of dbcot to the metal.

The redox properties of  $1^+$  and  $2^+$  were investigated using cyclic voltammetry. All complexes reveal reversible one-electron oxidation waves in the scan range between 10 and 200 mV/s. The redox potential of the bla rhodium complex is higher by 47 mV compared to the iridium analogue, which is in line with previous results showing that a variety of  $[\text{Ir}(\text{cod})(\text{N}_3\text{-ligand})]^+$  (cod = 1,5-cyclooctadiene) complexes are oxidized at lower potentials than their rhodium analogues ( $E_{1/2}$  lowered by 70–100 mV in those cases).<sup>11</sup>

**Synthesis and Characterization of Paramagnetic  $[\text{M}^{\text{II}}(\text{dbcot})\text{-}(\text{bla})]^{2+}$  Complexes.** In contrast to the abundant chemistry of  $d^8$ -metal olefin complexes, well-characterized, stable  $d^7$  rhodium-(II) and iridium(II) olefin compounds are rather scarce.<sup>25</sup> This is caused by the general low stability of organometallic radicals, coupled with relatively easy allylic C–H bond activation<sup>11,26</sup> and  $\text{C}_{\text{alkene}}\text{--C}_{\text{alkene}}$  coupling<sup>27</sup> reactions triggered by the open-shell metal center. We expected that the use of robust dbcot diolefin should block the undesired decomposition pathways involving the metal center and allow for exclusive reactivity on the nitrogen atom of the coordinated bislutidylamine.

The electrochemical data suggest that stable  $d^7$   $\text{M}^{\text{II}}$  complexes should be obtainable from  $1^+$  and  $2^+$  by one-electron oxidation. Hence we investigated their chemical oxidation in solution. Treatment of  $1^+$  and  $2^+$  with appropriate oxidants<sup>28</sup> led to formation of  $1^{2+}$  and  $2^{2+}$ , respectively (Scheme 5). Compound  $2^{2+}$  proved to be sufficiently stable to obtain X-ray quality crystals by layering an acetone solution of  $2^{2+}$  onto dichloromethane at  $-20^\circ\text{C}$ .

One-electron oxidation of  $2^+$  to  $2^{2+}$  results in a change of the coordination geometry from trigonal bipyramidal to a distorted square pyramid (*sqpy*) with the two lutidyl donors and the two olefinic double bonds coordinated in the basal plane and the amine at the apical position, as evidenced by the single-crystal X-ray diffraction (Figure 3). The Ir–N1 and Ir–N2 distances of  $2^{2+}$  are not significantly different ( $\Delta r < 3\sigma$ ). The same is observed for the distance between iridium and the olefinic bonds. Lower electron density on the metal after oxidation results in increased Ir–N and decreased Ir–olefin interactions as compared to  $2^+$ . The N1, N2 atoms and the centroids of the double bonds are not in one plane due to a slight “twist” of the dbcot moiety (Figure 3B). The measured crystal contained two independent molecules: the first isomer has the dbcot moiety twisted clockwise, whereas the other counterclockwise. Optimization of the X-ray structure using DFT resulted in convergence to a structure where N1, N2, and the centroids of the double bonds are aligned in a plane. The slightly “twisted” geometry thus seems to be a result of the crystal-packing forces.

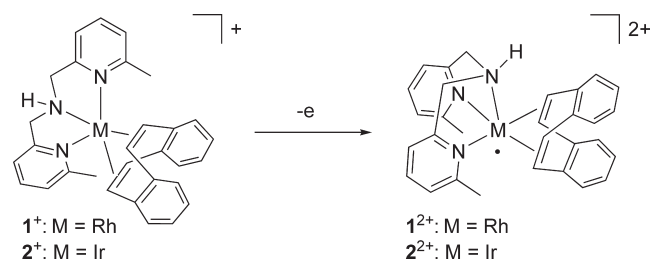
The observed change of the coordination geometry from *tbpy* to *sqpy* is more frequently observed when the electron configuration of the transition metal changes from  $d^8$  to  $d^7$  and is most likely a result of the Jahn–Teller effect.<sup>29</sup> For that reason we expect that compound  $1^{2+}$  has a structure similar to  $2^{2+}$ .

We used EPR spectroscopy to further investigate the (electronic) structure of  $1^{2+}$  and  $2^{2+}$ . Measured X-band EPR spectra of  $1^{2+}$  and  $2^{2+}$  in frozen acetone could be simulated as rhombic spectra (i.e.,  $g_1 \neq g_2 \neq g_3$ ) with well-resolved (super)hyperfine interactions with the metal center and a single nitrogen atom along the  $g_3(z)$  axis (Figure 4 and Table 3). The measured  $g$  values are indicative of metal-centered radicals. As expected for heavier transition metals with larger spin–orbit couplings, the  $g$ -anisotropy (rhombicity) of the iridium complex  $2^{2+}$  is larger than that of the rhodium analogue  $1^{2+}$ .



Table 1. Selected Bond Distances (Å) and Angles (deg) for Complexes  $1^+$ ,  $2^+$ , and  $2^{2+}$ 

	$[\text{Rh}(\kappa^3\text{-bla})(\eta^4\text{-dbcot})]^+$		$[\text{Ir}(\kappa^3\text{-bla})(\eta^4\text{-dbcot})]^+$	$[\text{Ir}(\kappa^3\text{-bla})(\eta^4\text{-dbcot})]^{2+}$	
	$1a^+$	$1b^+$	$2^+$	$2a^{2+}$	$2b^{2+}$
M–N1	2.116(2)	2.113(2)	2.114(4)	2.111(3)	2.093(3)
M–N2	2.257(3)	2.259(3)	2.229(3)	2.095(3)	2.112(3)
M–N3	2.261(3)	2.249(3)	2.224(4)	2.184(3)	2.185(3)
M–C1	2.103(3)	2.101(3)	2.066(4)	2.189(3)	2.189(4)
M–C2	2.064(3)	2.062(3)	2.130(5)	2.159(3)	2.182(4)
M–C5	2.139(3)	2.147(3)	2.128(4)	2.191(3)	2.165(3)
M–C6	2.155(4)	2.155(4)	2.097(4)	2.184(4)	2.183(4)
C1–C2	1.440(5)	1.436(5)	1.472(6)	1.414(5)	1.410(5)
C5–C6	1.397(5)	1.400(5)	1.411(6)	1.390(5)	1.408(5)
C1–M–C2	40.42(13)	40.34(13)	41.41(17)	37.94(12)	37.65(13)
C5–M–C6	37.96(14)	37.99(14)	38.72(17)	37.05(13)	37.77(13)
N1–M–N2	88.97(9)	89.12(10)	91.48(12)	92.17(11)	89.91(11)
N1–M–N3	75.63(10)	75.00(9)	75.09(13)	76.57(11)	79.80(11)
N2–M–N3	76.18(10)	76.46(10)	76.55(12)	79.97(11)	76.93(12)

Scheme 5. Synthesis of Open-Shell Species  $[\text{Rh}(\eta^4\text{-dbcot})(\kappa^3\text{-bla})]^{2+}$  ( $1^{2+}$ ) and  $[\text{Ir}(\eta^4\text{-dbcot})(\kappa^3\text{-bla})]^{2+}$  ( $2^{2+}$ )

The spectrum of the iridium(II) compound  $2^{2+}$  is influenced by the presence of large Ir-quadrupole interactions, causing the appearance of two weak “forbidden” transitions, as indicated by the arrows in Figure 4.<sup>11,30</sup> Since the spectrum does not reveal any resolved hyperfines in this region of the spectrum that could be influenced by these quadrupole interactions, we did not take these interactions into account in the spectral simulations.

To get a better insight in the electronic structure of both complexes, we calculated the EPR properties with DFT (Table 3). In line with the experiments, DFT predicts that  $1^{2+}$  and  $2^{2+}$  are metal-centered radicals with Mulliken spin densities of about 72% and 73% on rhodium and iridium, respectively, and around 16.5% on the amine nitrogen atom.

The radical species  $1^{2+}$  and  $2^{2+}$  are sterically shielded around the metal, which is reflected by their relative inertness toward dioxygen in solution. Bubbling air through the solutions of  $1^{2+}$  or  $2^{2+}$  did not give rise to formation of superoxo species nor to a noticeable decrease of the EPR signal. Apparently, the shielding of the metal center by the methyl groups of the bla ligand prevents any rapid radical-type reactivity at the metal center. However, somewhat surprisingly, in solution the complexes slowly convert to the one-electron-reduced diamagnetic compounds  $1^+$  and  $2^+$ , as evidenced by NMR spectroscopy.<sup>31</sup> This process is not a disproportionation reaction (as commonly observed for  $\text{Rh}^{\text{II}}$  and  $\text{Ir}^{\text{II}}$  complexes),

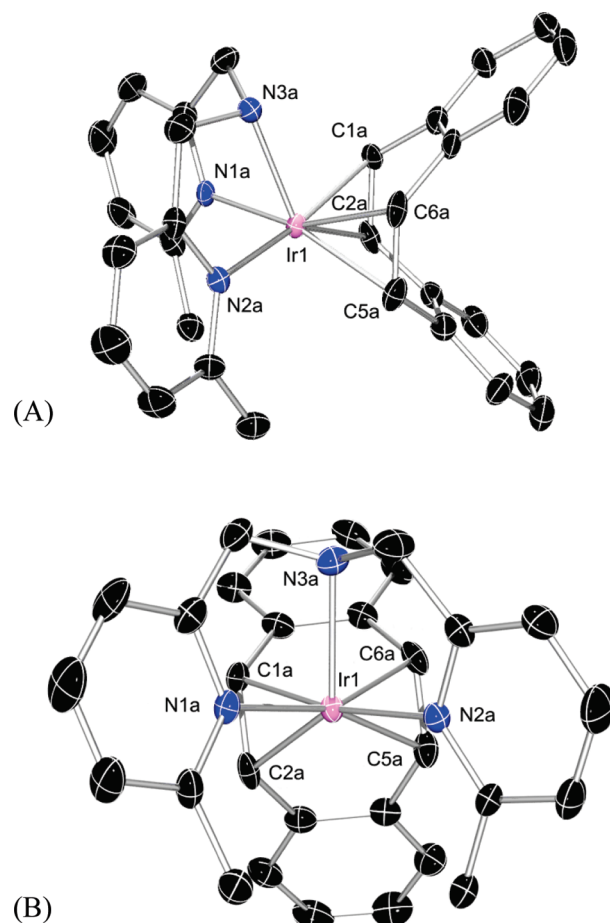
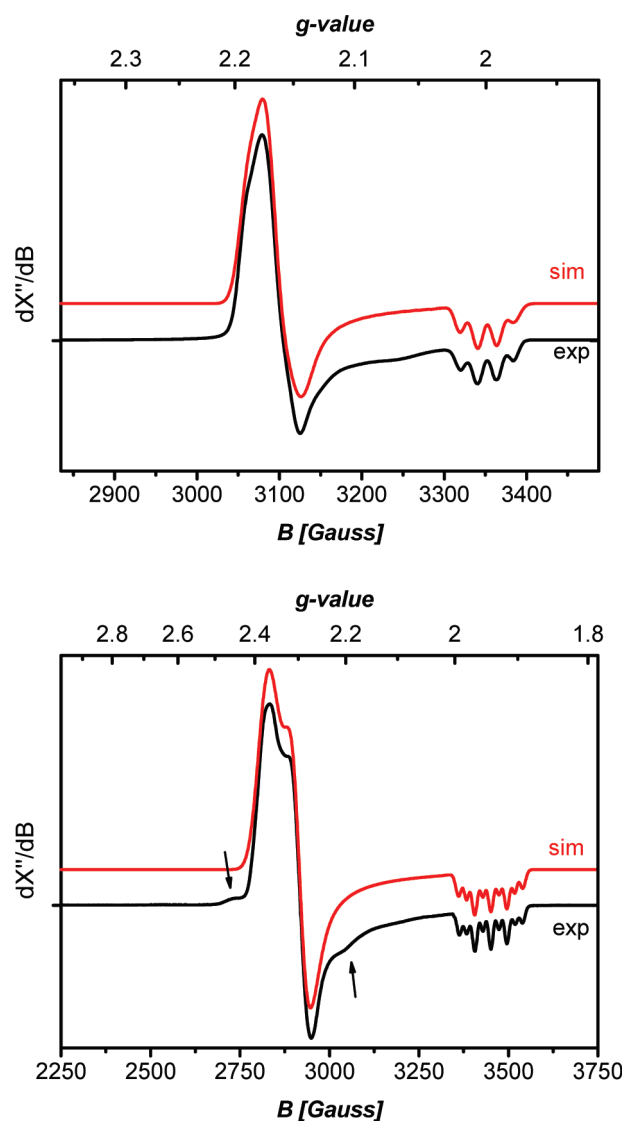


Figure 3. X-ray structure of  $[\text{Ir}(\eta^4\text{-dbcot})(\kappa^3\text{-bla})]^{2+}$  ( $2^{2+}$ ). Displacement ellipsoids are drawn at the 50% probability level (hydrogen atoms, the  $\text{PF}_6^-$  counterions, and a disordered  $\text{CH}_2\text{Cl}_2$  molecule are omitted for clarity). The crystal contains two independent cations in the asymmetric unit; only one of them is shown. See Table 1 for selected bond distances and angles.

because the one-electron-reduced species  $1^+$  and  $2^+$  are the only observed products.



**Figure 4.** Experimental and simulated X-band EPR spectra of  $[\text{Rh}^{\text{II}}(\text{dbcot})(\text{bla})]^{2+}$  (frequency: 9.379235 GHz; modulation amplitude: 0.8 G; power: 0.02 mW) complex  $1^{2+}$  (top) and  $[\text{Ir}^{\text{II}}(\text{dbcot})(\text{bla})]^{2+}$  (frequency 9.377560 GHz; modulation amplitude: 4 G; power: 0.2 mW) complex  $2^{2+}$  (bottom) recorded in frozen acetone at 60 K. Arrows indicate the forbidden transitions. The salt  $[n\text{-Bu}_4\text{N}]\text{PF}_6$  was added to the solution to obtain a better glass. The spectrum of  $4^{2+}$  is similar to the spectrum of  $1^{2+}$  (see Supporting Information).

Our initial hypothesis was that the increased charge of the metal (changing from  $1+$  to  $2+$  upon one-electron oxidation) results in an increased acidity of the NH group of the bla ligand. Spontaneous deprotonation of the amine group would then lead to formation of an aminyl radical via an *intramolecular* redox reaction between the metal and the nitrogen atom. Subsequently, this aminyl radical could then abstract a hydrogen atom from the reaction medium, thus re-forming the reduced complex  $1^+$  or  $2^+$  (Scheme 6). To check whether the re-formation of compounds  $1^+$  and  $2^+$  indeed proceeds via the pathway shown in Scheme 6, we studied the reactivity of  $1^{2+}$  and  $2^{2+}$  toward Brønsted bases.

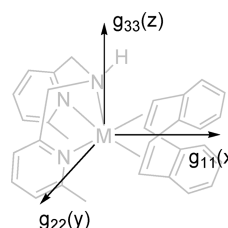
Reaction of complexes  $1^{2+}$  and  $2^{2+}$  with solid  $\text{K}_2\text{CO}_3$  in acetone or acetonitrile resulted in disappearance of the characteristic EPR signals, and no signal of the putative aminyl radical

**Table 2.** Electrochemical Data for Complexes  $1^+$ ,  $2^+$ , and  $4^+$  (*vide supra*)<sup>a</sup>

complex	$E_a$ (V)	$\Delta E$ (mV)	$E_{1/2}$ (V)	$I_f/I_b$
$[\text{Rh}(\eta^4\text{-dbcot})(\kappa^3\text{-bla})]\text{PF}_6$ ( <b>1</b> ) $\text{PF}_6$	0.410	101	0.359	1.0
$[\text{Ir}(\eta^4\text{-dbcot})(\kappa^3\text{-bla})]\text{PF}_6$ ( <b>2</b> ) $\text{PF}_6$	0.364	104	0.312	1.0
$[\text{Rh}(\eta^4\text{-dbcot})(\kappa^3\text{-Bn-bla})]\text{PF}_6$ ( <b>4</b> ) $\text{PF}_6$	0.477	70	0.443	1.0

<sup>a</sup> Solvent:  $\text{CH}_2\text{Cl}_2$ ; scan rate = 40 mV/s;  $E_{1/2}$  vs  $\text{Fc}/\text{Fc}^+$ .  $\Delta E$  = peak separation,  $E_a$  = anodic peak potential,  $E_{1/2}$  = half-wave potential,  $I_f/I_b$  = anodic peak current/cathodic peak current.

**Table 3.** Simulated (expt) and Calculated (DFT)  $g$  Values and (Super)hyperfine Interactions (MHz) for Compounds  $1^{2+}$ ,  $2^{2+}$ , and  $4^{2+}$

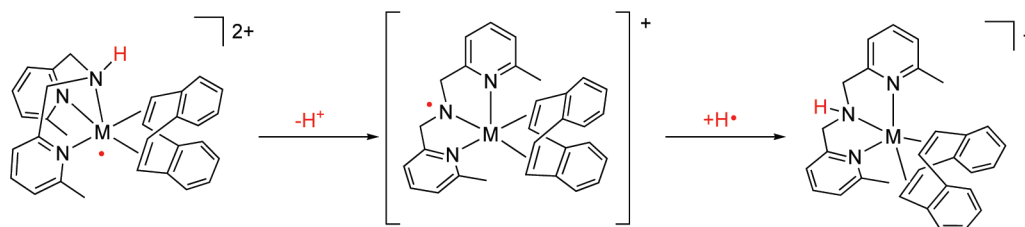
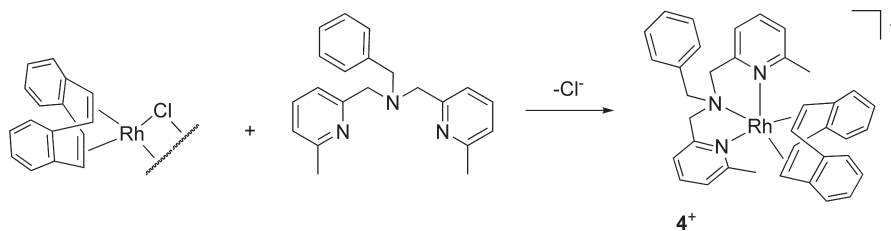


complex	property	$g_{11}(x)$		$g_{22}(y)$		$g_{33}(z)$	
		expt	DFT	expt	DFT	expt	DFT
$1^{2+}$	g value	2.181	2.133	2.158	2.118	2.000	1.982
	$\text{HFI}_{\text{Rh}}$	n.r.	-7.67	n.r.	-14.2	54.0	-74.6
	$\text{HFI}_{\text{N}}$	n.r.	36.8	n.r.	36.9	64.0	62.1
$2^{2+}$	g value	2.368	2.320	2.294	2.257	1.942	1.863
	$\text{HFI}_{\text{Ir}}$	n.r.	97.0	n.r.	103	122.0	167
	$\text{HFI}_{\text{N}}$	n.r.	38.4	n.r.	38.5	60.0	63.2
$4^{2+}$	g value	2.211	2.128	2.184	2.122	1.996	1.982
	$\text{HFI}_{\text{Rh}}$	n.r.	-8.67	n.r.	-16.9	58.9	-70.7
	$\text{HFI}_{\text{N}}$	n.r.	34.1	n.r.	34.2	61.8	63.3

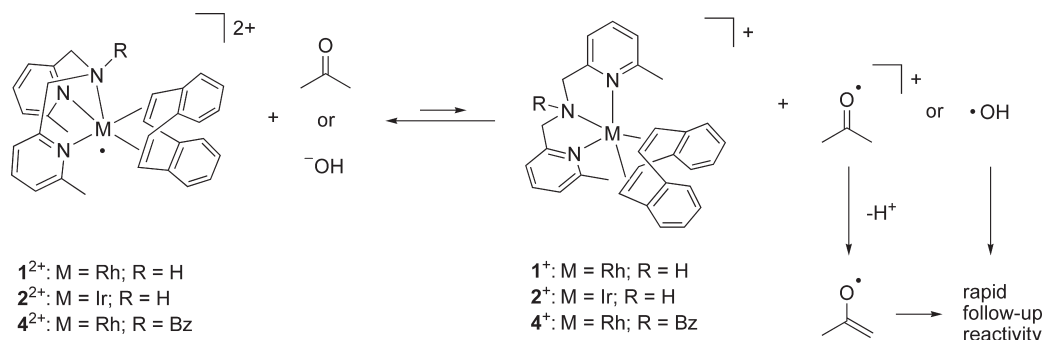
<sup>a</sup> n.r. = not resolved. Directions of the principal axes of the  $g$ -tensor in the molecular axis system of complexes are shown.

could be detected.<sup>32</sup> Instead, quantitative formation of the one-electron-reduced diamagnetic complexes  $1^+$  and  $2^+$  was observed with  $^1\text{H}$  NMR. Remarkably, the NMR data further reveal that the reactions retain the N-H hydrogen atoms for a large part, whereas formation of the N-D deuterated analogues of  $1^+$  and  $2^+$  would be expected if the reactions would proceed via the pathway depicted in Scheme 6. This makes the aminyl radical pathway rather doubtful, unless the reaction would be associated with a very large kinetic isotope effect.<sup>33</sup> Radical trapping experiments<sup>34</sup> did not allow for unambiguous detection of the proposed aminyl radicals nor of solvent radicals.<sup>35</sup>

**Synthesis of Paramagnetic N-Protected  $[\text{Rh}^{\text{II}}(\text{Bn-bla})(\text{dbcot})]^{2+}$  Complex and Its Reactivity with  $\text{K}_2\text{CO}_3$ .** Since the above results are inconclusive about the role of the amine/aminyl radical in the observed reduction of  $1^{2+}/2^{2+}$  to  $1^+/2^+$ , we decided to perform a control experiment using a similar compound in which the amine is protected with a benzyl moiety. Hence we investigated the reactivity of the complex  $[\text{Rh}(\text{dbcot})(\text{Bn-bla})](\text{PF}_6)_2$  (**4**) $(\text{PF}_6)_2$ .

Scheme 6. Hypothetical Deprotonation–HAT Pathway Leading to Net Reduction of the Paramagnetic Species  $1^{2+}$  and  $2^{2+}$ Scheme 7. Synthesis of  $[\text{Rh}(\eta^4\text{-dbcot})(\kappa^3\text{-Bn-bla})]^+$  ( $4^+$ )

Scheme 8. Regeneration of the Diamagnetic Complex by Base-Promoted Oxidation of Solvent or Hydroxide Anion



The precursor complex  $[\text{Rh}(\eta^4\text{-dbcot})(\kappa^3\text{-Bn-bla})]\text{PF}_6$  ( $[4]\text{PF}_6$ ) was prepared using the method described for  $[1]\text{PF}_6$  (Scheme 7). The  $^1\text{H}$  NMR signals of the dbcot moiety in compound  $4^+$  are broadened compared to the signals of Bn-bla at room temperature, and contrary to  $1^+$  and  $2^+$  the olefinic signals of dbcot are magnetically inequivalent, giving two broad signals at 4.75 and 4.24. This suggests that the rotation of dbcot is much slower in the case of  $4^+$  than in  $1^+$  and  $2^+$ .

CV measurements reveal that the redox potential of  $[\text{Rh}(\text{Bn-bla})(\text{dbcot})]^+$  ( $4^+$ ) is higher by 67 and 170 mV compared with  $[\text{Rh}(\text{bla})(\text{dbcot})]^+$  ( $1^+$ ) and the previously reported  $[\text{Rh}(\text{Bn-bla})(\text{cod})]^+$ ,<sup>11</sup> respectively, showing that exchange of either the bla ligand for the Bn-bla ligand or cod for dbcot results in a considerable destabilization of the +II oxidation state of rhodium (see Table 2). For that reason we used  $\text{AgPF}_6$  in DCM as the oxidizing reagent to form  $4^{2+}$ .

The EPR spectrum of  $4^{2+}$  (see the Supporting Information) is very similar to the spectrum of  $1^{2+}$  and shows a rhombic, almost axial  $g$ -tensor and hyperfine couplings with rhodium and nitrogen (see Table 3). As for  $1^{2+}$  and  $2^{2+}$  the DFT-calculated EPR parameters are in good qualitative agreement with the experiment. The DFT-calculated Mulliken spin densities at rhodium (67%) and nitrogen (18%) are comparable to those of  $1^{2+}$  and  $2^{2+}$ .

Stirring an acetone- $d_6$  solution of  $4^{2+}$  (directly dissolved from a pregenerated 1:1 mixture of  $4^{2+}$  and precipitated metallic silver) with solid  $\text{K}_2\text{CO}_3$  again results in a color change from dark green to bright yellow, with quantitative formation of the reduced species  $4^+$  (as evidenced by NMR). This is similar to the reactions observed for  $1^{2+}$  and  $2^{2+}$  and shows that the presence of the N–H group is not necessary for the reduction of the  $\text{M}^{\text{II}}$  oxidation state radical species to their  $\text{M}^{\text{I}}$  precursors. Hence, the reaction does not necessarily involve the intermediacy of aminyl radicals, and the role of the Brønsted base has to be different than originally anticipated.

Base-assisted oxidation of solvent<sup>36</sup> seems to be a viable pathway for the reduction of species  $1^{2+}/2^{2+}$  (Scheme 8).<sup>37</sup> Judging from the redox potentials, the dicationic radical metal complexes  $1^{2+}/2^{2+}$  and acetone must exist in a redox equilibrium with the closed-shell metal complexes  $1^+/2^+$  and the acetone radical cation.<sup>38</sup> Without a base, this equilibrium lies far to the left, but the acetone radical cation formed in small quantities can be easily deprotonated by the base, shifting the redox equilibrium between acetone and  $1^{2+}/2^{2+}$  completely to the right. Alternatively, in the presence of small quantities of water the hydroxide anion can be generated, which is known as a potential one-electron reducing agent in organic solvents.<sup>39</sup>

Table 4. Crystallographic Data for [1](PF<sub>6</sub>), [2](PF<sub>6</sub>), [2](PF<sub>6</sub>)<sub>2</sub>, and [3](PF<sub>6</sub>)

	[Rh( $\kappa^3$ -bla) (dbcot)]PF <sub>6</sub> ·CH <sub>3</sub> COCH <sub>3</sub> ([1]PF <sub>6</sub> )	[Ir( $\kappa^3$ -bla)(dbcot)]PF <sub>6</sub> · (CH <sub>3</sub> CH <sub>2</sub> ) <sub>2</sub> O ([2]PF <sub>6</sub> )	[Ir( $\kappa^3$ -bla)(dbcot)](PF <sub>6</sub> ) <sub>2</sub> · CH <sub>2</sub> Cl <sub>2</sub> ([2](PF <sub>6</sub> ) <sub>2</sub> )	[Ir( $\kappa^3$ -bla)(H)( $\sigma$ -C <sub>8</sub> H <sub>13</sub> ) ( $\eta^2$ -C <sub>8</sub> H <sub>14</sub> )]PF <sub>6</sub> (3[PF <sub>6</sub> ])
empirical formula	C <sub>30</sub> H <sub>29</sub> N <sub>3</sub> Rh, C <sub>3</sub> H <sub>6</sub> O, F <sub>6</sub> P	C <sub>30</sub> H <sub>29</sub> IrN <sub>3</sub> , C <sub>4</sub> H <sub>10</sub> O, F <sub>6</sub> P	2(C <sub>30</sub> H <sub>29</sub> IrN <sub>3</sub> ), 4(F <sub>6</sub> P), CH <sub>2</sub> Cl <sub>2</sub> + solvent	C <sub>30</sub> H <sub>45</sub> IrN <sub>3</sub> , F <sub>6</sub> P
fw	737.52	842.87	1912.37 <sup>a</sup>	784.88
temperature [K]	110	110	110	150
radiation	Mo K $\alpha$	Mo K $\alpha$	Mo K $\alpha$	Mo K $\alpha$
wavelength [Å]	0.71073	0.71073	0.71073	0.71073
cryst syst	monoclinic	monoclinic	monoclinic	monoclinic
space group	Cc	P21/c	P21/c	P21/c
a [Å]	28.5187(8)	9.2911(4)	21.5483(9)	9.5523(7)
b [Å]	11.2036(3)	20.4418(9)	16.7416(7)	16.2517(5)
c [Å]	19.4833(4)	17.3595(7)	20.9573(8)	20.1842(7)
$\beta$ [deg]	101.351(1)	98.599(2)	110.520(2)	97.861(2)
volume [Å <sup>3</sup> ]	6103.4(3)	3260.0(2)	7080.7(5)	3104.0(3)
Z	8	4	4	4
color	yellow	yellow	black	pale yellow
$\theta$ -max	27.5	27.5	27.5	27.5
density [Mg m <sup>-3</sup> ]	1.605	1.717	1.794 <sup>a</sup>	1.680
absorp coeff [mm <sup>-1</sup> ]	0.682	4.212	4.027 <sup>a</sup>	4.414
F(000)	3008	1672	3728 <sup>a</sup>	1568
R <sub>1</sub> /wR <sub>2</sub> /S	0.0281/0.0600/1.047	0.0333/0.0584/1.093	0.0292/0.0759/1.101	0.0234/0.0496/1.027

<sup>a</sup> Excluding the disordered solvent contribution.

Thus, depending on the water content in the solvent (or base), this seems to be a plausible mechanism as well.

At this point we cannot exclude that the pathway involving deprotonation of the N–H group can take place, taking into account the reactivity of related amine complexes of rhodium and iridium. Instant hydrogen atom abstraction by an iridium-coordinated aminyl radical has been recently reported by Grützmacher et al.<sup>15c</sup> However, it is tempting to assume that base-assisted solvent oxidation is the actual mechanism of re-formation of **1**<sup>+</sup>/**2**<sup>+</sup> from **1**<sup>2+</sup>/**2**<sup>2+</sup> and that the aminyl radical pathway plays little (if any) role in this reaction.

## SUMMARY AND CONCLUSIONS

Open-shell rhodium(II) and iridium(II) complexes with dibenzocyclooctadiene (dbcot)- and bislutidylamine (bla)-type ligands were successfully synthesized. They represent rare examples of isolable open-shell olefin complexes. The chosen diolefin ligand is inert to radical reactions, which allowed for investigations of possible radical reactivity pathways involving the aminyl nitrogen atom of the bla ligand.

An attempt to obtain the aminyl radical complexes by deprotonation of the N–H group of the bla ligand using a base led to an unexpected, selective reduction of the paramagnetic species [M<sup>II</sup>(dbcot)(bla)]<sup>2+</sup> to their one-electron-reduced closed-shell analogues [M<sup>I</sup>(dbcot)(bla)]<sup>+</sup> (M = Rh, Ir). Control experiments with the rhodium(II) complex [Rh<sup>II</sup>(dbcot)(Bn-bla)]<sup>2+</sup> containing the Bn-bla ligand (a bla derivative having the amine protected with a benzyl group) revealed similar reactivity.

These results show that the generation of aminyl radicals from the complexes of the general formula [M<sup>II</sup>(diolefin)(N<sub>3</sub>-ligand)]<sup>2+</sup> (M = Rh, Ir) is perhaps not occurring at all. At least it is rather unlikely that the observed reduction reactions occur

via deprotonation of the amine followed by HAT. It is remarkable, however, that the complexes studied are quantitatively reduced in the presence of bases to the M<sup>I</sup> species. The reduction is most likely caused by a hydroxide anion or a solvent molecule that can be deprotonated in its oxidized form. We show that generation of aminyl radicals at cationic rhodium(II) and iridium(II) species is not as straightforward as expected. Deprotonation of amines coordinated to these paramagnetic metal centers might well be intrinsically limited by the instability of the reactive radical compounds under basic conditions. Generation of aminyl radicals on bislutidylamine ligands (or bispicolyl-type ligands in general) remains elusive.

## EXPERIMENTAL SECTION

**X-ray Diffraction.** X-ray data were collected at low temperature under the control of the Nonius COLLECT software with a Nonius KappaCCD on a rotating anode. Numerical details have been collected in Table 4. The structures are shown in Figures 1, 2, and 3.<sup>40</sup> The intensity data were corrected for absorption with the program SADABS. The structures were solved with the program DIRDIF and refined with SHELXL97. The Flack parameter for [1]PF<sub>6</sub> refined to 0.484(13) with a BASF/TWIN refinement. The structure of [2](PF<sub>6</sub>)<sub>2</sub> has solvent-accessible voids filled with disordered solvent. Their contribution to the structure factors in the refinement was taken into account with the PLATON/SQUEEZE approach. The hydrogen atom on Ir for [3]PF<sub>6</sub> was located in a difference density map.

**DFT Calculations.** Geometry optimizations were carried out with the Turbomole program package<sup>41</sup> coupled to the PQS Baker optimizer<sup>42</sup> at the ri-DFT<sup>43</sup> level using the BP86<sup>44</sup> functional and SV(P) basis set.<sup>45</sup> Calculated EPR spectra<sup>46</sup> were obtained with the ADF program<sup>47</sup> at the DFT, BP86,<sup>48</sup> and TZP<sup>49</sup> level, using the Turbomole-optimized geometries.



**General Procedures.** All manipulations were performed in an argon atmosphere by standard Schlenk techniques or in a glovebox. Methanol, acetonitrile, and dichloromethane were distilled under nitrogen from CaH<sub>2</sub>. Hexanes were distilled under nitrogen from Na wire. Acetone was deoxygenated using the freeze–pump–thaw method. NMR experiments were carried out on a Bruker DRX300 (300 and 75 MHz for <sup>1</sup>H and <sup>13</sup>C, respectively) or on a Varian Inova 500 (500 and 125 MHz for <sup>1</sup>H and <sup>13</sup>C, respectively) spectrometer. Solvent shift reference: acetone-*d*<sub>6</sub> δ = 2.05 and δ = 29.84 for <sup>1</sup>H and <sup>13</sup>C, CDCl<sub>3</sub> δ = 7.26 and δ = 77.16 for <sup>1</sup>H and <sup>13</sup>C, respectively. Abbreviations used are s = singlet, d = doublet, t = triplet, m = multiplet, br = broad. Elemental analyses (CHN) were carried out by H. Kolbe Mikroanalytisches Laboratorium (Germany). X-band EPR spectroscopy measurements were performed with a Bruker EMX Plus spectrometer. Cyclic voltammograms of ~2 mM parent compounds in 1 M Bu<sub>4</sub>NPF<sub>6</sub> electrolyte solution were recorded in a gastight single-compartment three-electrode cell equipped with platinum working (apparent surface of 0.42 mm<sup>2</sup>), coiled platinum wire auxiliary, and silver wire pseudoreference electrodes. The cell was connected to a computer-controlled PAR model 283 potentiostat. All redox potentials are reported against the ferrocene/ferrocenium (Fc/Fc<sup>+</sup>) redox couple. Ferrocene was used as internal standard. Magnetic susceptibility was measured on a Magway MSB Mk1 magnetic balance. [Fe(μ-C<sub>5</sub>H<sub>4</sub>COMe)Cp]PF<sub>6</sub>,<sup>28</sup> [Ir(dbcot)(μ-Cl)]<sub>2</sub>,<sup>50</sup> [M(coe)<sub>2</sub>(μ-Cl)]<sub>2</sub>,<sup>51</sup> dibenzo[*a,e*]cyclooctatetraene,<sup>52</sup> *N*-benzyl-*N,N*-di[(6-methyl-2-pyridylmethyl)]amine,<sup>53</sup> and bis[(6-methyl-2-pyridyl)methyl]amine<sup>54</sup> have been prepared according to previously reported procedures.

**Dibenzo[*a,e*]cyclooctadiene.** Although various experimental procedures are available for the synthesis of dbcot,<sup>52</sup> we did not find a full assignment of all <sup>13</sup>C NMR signals of this compound. <sup>1</sup>H NMR (500 MHz, CDCl<sub>3</sub> (7.26 ppm)): δ 7.17 (m, 4H, Ar<sub>dbcot</sub>-H); 7.08 (m, 4H, Ar<sub>dbcot</sub>-H); 6.78 (s, 4H, olefinic). <sup>13</sup>C NMR (125 MHz, CDCl<sub>3</sub> (77.23 ppm)): δ 137.27 (C<sup>IV</sup>); 133.44 (olefinic); 129.31; 127.03.

**Synthesis of [Rh(κ<sup>3</sup>-bla)(dbcot)]PF<sub>6</sub> ([1]PF<sub>6</sub>).** [Rh(coe)<sub>2</sub>Cl]<sub>2</sub> (179 mg, 0.499 mmol Rh) and 107 mg of dbcot (0.524 mmol) were dissolved in 10 mL of CH<sub>2</sub>Cl<sub>2</sub>, and the solution was stirred for 2 h and evaporated to dryness. Next, 115 mg of bla (0.506 mmol) and a mixture of 10 mL of MeOH and 10 mL of CH<sub>2</sub>Cl<sub>2</sub> were added and stirred for 1 h. The unreacted solid was filtered off, and the remaining solvent was removed *in vacuo*. The thus formed solid was dissolved in 5 mL of MeOH, and 106 mg of KPF<sub>6</sub> was added, causing precipitation of a bright yellow solid, which was filtered and washed with 2 mL of MeOH. Yield: 168 mg (0.247 mmol, 49.5%).

<sup>1</sup>H NMR (500 MHz, acetone-*d*<sub>6</sub>): δ 7.80 (t, <sup>3</sup>J(H,H) = 7.5 Hz, 2H; Py); 7.44 (d, <sup>3</sup>J(H,H) = 7.5 Hz, 2H; Py); 7.35 (d, <sup>3</sup>J(H,H) = 7.5 Hz, 2H; Py); 6.62 (m, 8H; Ar<sub>dbcot</sub>); 5.29 (d[AB] br, <sup>2</sup>J(H,H) = 15.5 Hz, 2H; N-CH<sub>2</sub>-Py); 4.50 (d, <sup>2</sup>J(Rh,H) = 1.5 Hz, 4H; CH=CH); 4.28 (d[AB], <sup>2</sup>J(H,H) = 16.5 Hz, 2H; N-CH<sub>2</sub>-Py); 3.39 (s br, 6H; Py-CH<sub>3</sub>). <sup>13</sup>C NMR (125 MHz, acetone-*d*<sub>6</sub>): δ 161.3 (Py); 161.2 (Py); 145.6 (Ar<sub>dbcot</sub>); 139.3 (Py-C4); 126.9 (Ar<sub>dbcot</sub>); 126.7 (Ar<sub>dbcot</sub>); 126.0 (Py-C5); 121.3 (Py-C3); 74.6 (d, <sup>2</sup>J(Rh,H) = 12.6 Hz; CH=CH); 58.3 (N-CH<sub>2</sub>-Py); 28.6 (Py-CH<sub>3</sub>). Anal. Calcd: C, 53.03; H, 4.30; N, 6.18; Found: 52.77; H, 4.67; N, 5.98.

**Synthesis of [Ir(κ<sup>3</sup>-bla)(dbcot)]PF<sub>6</sub> ([2]PF<sub>6</sub>).** [Ir(dbcot)Cl]<sub>2</sub> (300 mg, 0.695 mmol Ir) was suspended in 10 mL of methanol, and 160 mg of bla (0.704 mmol) was added. The solution was stirred for 30 min and turned transparent yellow. Then 128 mg KPF<sub>6</sub> (0.695 mmol) was added, causing precipitation of a bright yellow solid, which was filtered and washed with 2 mL of MeOH. Yield: 234 mg (0.304 mmol, 43.7%).

<sup>1</sup>H NMR (500 MHz, acetone-*d*<sub>6</sub>): δ 7.88 (t, <sup>3</sup>J(H,H) = 7.5 Hz, 2H; Py); 7.52 (d, <sup>3</sup>J(H,H) = 7.5 Hz, 2H; Py); 7.48 (d, <sup>3</sup>J(H,H) = 7.5 Hz, 2H; Py); 6.91 (m, 4H; Ar<sub>dbcot</sub>); 6.79 (m, 4H; Ar<sub>dbcot</sub>); 5.33 (d[AB], <sup>2</sup>J(H,H) = 17.0 Hz, 2H; N-CH<sub>2</sub>-Py); 4.52 (d[AB], <sup>2</sup>J(H,H) = 17 Hz, 2H; N-CH<sub>2</sub>-Py); 4.37 (s, 4H; CH=CH); 3.30 (s, 6H; Py-CH<sub>3</sub>). <sup>13</sup>C NMR (125 MHz, acetone-*d*<sub>6</sub>): δ 162.9 (Py); 161.5 (Py); 148.2 (Ar<sub>dbcot</sub>); 139.7 (Py-

C4); 127.2 (Ar<sub>dbcot</sub>); 126.5 (Py-C5); 126.4 (Ar<sub>dbcot</sub>); 121.5 (Py-C3); 60.2 (N-CH<sub>2</sub>-Py); 58.3 (CH=CH); 29.5 (Py-CH<sub>3</sub>). Anal. Calcd for [2]PF<sub>6</sub>·CH<sub>3</sub>OH: C, 46.50; H, 4.15; N, 5.25. Found: C, 46.58; H, 4.29; N, 5.12. <sup>1</sup>H NMR indicates the presence of cocrystallized MeOH.

**Synthesis of [Rh(κ<sup>3</sup>-bla)(dbcot)](PF<sub>6</sub>)<sub>2</sub> ([1](PF<sub>6</sub>)<sub>2</sub>).** [1]PF<sub>6</sub> (94.5 mg, 0.139 mmol) and 35.6 mg of AgPF<sub>6</sub> (0.141 mmol) were dissolved in 3 mL of acetone and left to react for 30 min. The solution was filtered using a syringe filter, and the filtrate was condensed to a black oil *in vacuo*. An 8 mL amount of CH<sub>2</sub>Cl<sub>2</sub> was added, causing precipitation of a purple solid, which was centrifuged. Yield: 84 mg (0.102 mmol, 73.4%). Unfortunately, despite many attempts, due to the intrinsic instability of [1](PF<sub>6</sub>)<sub>2</sub>, we were not able to obtain an analytically pure sample.

**Synthesis of [Ir(κ<sup>3</sup>-bla)(dbcot)](PF<sub>6</sub>)<sub>2</sub>·CH<sub>2</sub>Cl<sub>2</sub> ([2](PF<sub>6</sub>)<sub>2</sub>).** [2]PF<sub>6</sub> (136 mg, 0.177 mmol) and 50 mg of [Fe(μ-C<sub>5</sub>H<sub>4</sub>COMe)Cp]PF<sub>6</sub> (0.15 mmol) were dissolved in 20 mL of dichloromethane and stirred for 45 min, at which time a brown precipitate formed and the characteristic absorbance of acetylferrocenium was gone. The solution was filtered, washed with dichloromethane, and dried *in vacuo*. Yield: 80 mg (0.08 mmol, 53.3%). Magnetic susceptibility: μ<sub>eff</sub> = 2.06 (corrected for diamagnetism of [2]PF<sub>6</sub>, PF<sub>6</sub>, Ir<sup>2+</sup>, and CH<sub>2</sub>Cl<sub>2</sub>; measured: 1.90).<sup>55</sup> Anal. Calcd for [2](PF<sub>6</sub>)<sub>2</sub>·CH<sub>2</sub>Cl<sub>2</sub>: C, 37.28; H, 3.13; N, 4.21. Found: C, 37.24; H, 3.08; N, 4.36.

**Synthesis of [Ir(κ<sup>3</sup>-bla)(H)(σ-C<sub>8</sub>H<sub>13</sub>)(η<sup>2</sup>-C<sub>8</sub>H<sub>14</sub>)]PF<sub>6</sub> ([3]PF<sub>6</sub>).** An excess of dbcot (238, 1.17 mmol) and bla (265 mg, 1.17 mmol) were added to a suspension of [Ir(coe)<sub>2</sub>Cl]<sub>2</sub> (523 mg, 1.16 mmol Ir) in dry methanol (40 mL), and the mixture was stirred for 18 h. The reaction mixture turned to a transparent green solution, to which NH<sub>4</sub>PF<sub>6</sub> was added, causing precipitation of a white solid. The product was filtered off and recrystallized. Yield: 270 mg, 30%. Crystals suitable for X-ray diffraction were grown by layering an acetone solution of 3[PF<sub>6</sub>] with hexanes.

<sup>1</sup>H NMR (acetone-*d*<sub>6</sub>, 300 MHz): δ 7.79 (t, <sup>3</sup>J(H,H) = 7.8 Hz, 1H; Py<sup>A</sup>); 7.63 (t, <sup>3</sup>J(H,H) = 7.5 Hz, 1H; Py<sup>B</sup>); 7.46 (m, 2H; Py<sup>A</sup>); 7.25 (d, <sup>3</sup>J(H,H) = 7.5 Hz, 2H; Py<sup>B</sup>); 6.60 (s, br, 1H; N-H); 5.47 (dd[AB], <sup>2</sup>J(H,H) = 17.7 Hz, <sup>3</sup>J(H,H) = 8.1 Hz, 1H; N-CH<sub>2</sub>-Py); 5.15 (dd[AB], <sup>2</sup>J(H,H) = 15.9 Hz, <sup>3</sup>J(H,H) = 5.1 Hz, 1H; N-CH<sub>2</sub>-Py); 5.05 (t, <sup>3</sup>J(H,H) = 7.5 Hz, 1H; Ir-C-H); 4.76 (dd[AB], <sup>2</sup>J(H,H) = 18.6 Hz, 1H; N-CH<sub>2</sub>-Py); 4.68 (dd[AB], <sup>2</sup>J(H,H) = 15.6 Hz, 1H; N-CH<sub>2</sub>-Py); 3.88 (m, 2H; CH=CH); 3.13 (s, 3H; Py<sup>A</sup>-CH<sub>3</sub>); 3.02 (s, 3H; Py<sup>B</sup>-CH<sub>3</sub>); 2.66 (m, 1H; coe); 2.25 (m, 1H; coe); 1.5 (m, 22H; coe); -15.84 (s, 1H, Ir-H). <sup>13</sup>C NMR (75 MHz, acetone-*d*<sub>6</sub>): δ 164.5 (Py); 163.4 (Py); 162.3 (Py); 161.7 (Py); 140.5 (Py<sup>A</sup>); 139.6 (Py<sup>B</sup>); 127.9 (IrC=CH); 127.5 (PyA); 127.2; (Ir-C); 125.6 (PyB); 122.1 (Py<sup>A</sup>); 121.6 (Py<sup>B</sup>); 69.3 (CH=CH); 64.6 (N-CH); 63.9 (N-CH) 63.8 (CH=CH); 40.8 (CH-CH<sub>2</sub>); 33.8 (CH-CH<sub>2</sub>); 33.1 (CH-CH<sub>2</sub>); 33.0 (CH-CH<sub>2</sub>); 32.4 (coe); 32.2 (Py<sup>A</sup>CH<sub>3</sub>); 31.8 (Py<sup>B</sup>CH<sub>3</sub>); 29.9 (coe); 29.7 (coe); 28.8 (coe); 28.5 (coe); 25.5 (coe); 27.8 (coe); 27.6 (coe). Anal. Calcd (C<sub>30</sub>H<sub>45</sub>F<sub>6</sub>IrN<sub>3</sub>P): C, 45.91; H, 5.78; N, 5.35. Found: C, 45.83; H, 5.86; N, 5.33

**Synthesis of [Rh(κ<sup>3</sup>-Bn-bla)(dbcot)]PF<sub>6</sub> ([4]PF<sub>6</sub>).** [Rh(coe)<sub>2</sub>Cl]<sub>2</sub> (180 mg, 0.499 mmol Rh) and 102 mg of dbcot (0.499 mmol) were dissolved in 10 mL of CH<sub>2</sub>Cl<sub>2</sub>, and the solution was stirred for 2 h and evaporated to dryness. Next, 164 mg of Bn-bla (0.517 mmol) and a mixture of 8 mL of MeOH and 8 mL of CH<sub>2</sub>Cl<sub>2</sub> were added and stirred for 1 h, and the solvent was removed *in vacuo*. The thus formed solid was dissolved in 6 mL of MeOH, and 126 mg of KPF<sub>6</sub> was added, causing precipitation of a bright yellow solid. Then 2 mL of H<sub>2</sub>O was added, and the solution was stirred for 15 min, after which it was filtered and washed with 2 mL of MeOH. Yield: 331 mg (0.430 mmol, 86.2%).

<sup>1</sup>H NMR (300 MHz, acetone-*d*<sub>6</sub>): δ 7.80 (t, <sup>3</sup>J(H,H) = 7.7 Hz, 2H; Py); 7.66–7.41 (m, 5H; Py, Ph); 7.36 (d, <sup>3</sup>J(H,H) = 7.6 Hz, 2H; Py); 7.03 (m, br, 4H; Ar<sub>dbcot</sub>); 6.97 (m, br, 4H; Ar<sub>dbcot</sub>); 5.04 (d[AB] br, <sup>2</sup>J(H,H) = 15.8 Hz, 2H; N-CH<sub>2</sub>-Py); 4.91 (s, 2H; N-CH<sub>2</sub>-Ph); 4.75 (s,

br, 4H;  $\text{CH}=\text{CH}$ ), 4.24 (s, br, 4H;  $\text{CH}=\text{CH}$ ); 3.86 (d[AB],  $^2J(\text{H,H}) = 16.0$  Hz, 2H; N- $\text{CH}_2$ -Py); 3.60 (s, 6H; Py- $\text{CH}_3$ ).  $^{13}\text{C}$  NMR (125 MHz, acetone- $d_6$ ):  $\delta$  162.1 (Py); 160.6 (Py); 145.0 ( $\text{Ar}_{\text{dbcot}}\text{-C1}$ ); 139.8 (Py-C4); 133.5 ( $\text{Ar}_{\text{dbcot}}\text{-C1}$ ); 132.7 (Ph-C2/6); 129.7 (Ph-C3/5); 129.7 (Ph-C4); 127.3 ( $\text{Ar}_{\text{dbcot}}\text{-C2/3}$ ); 127.2 (Py-C5); 122.6 (Py-C3); 63.6 (N- $\text{CH}_2$ -Ph); 61.6 (N- $\text{CH}_2$ -Py); 30.0 (Py- $\text{CH}_3$ ). The  $^{13}\text{C}$  NMR signals of the double bond of dbcot could not be located due to the fluxional behavior of this moiety. FAB $^+$ -MS: calcd for  $[\text{4}]^+$  ( $\text{C}_{37}\text{H}_{35}\text{N}_3\text{Rh}$ )  $m/z$  624.1883; found  $m/z$  624.1886 ( $\Delta = -0.5$  ppm).

**Synthesis of  $[\text{Rh}(\kappa^3\text{-Bn-bla})(\text{dbcot})](\text{PF}_6)_2$  ( $[\text{4}](\text{PF}_6)_2$ ).**  $[\text{4}](\text{PF}_6)_2$  (89.4 mg, 0.116 mmol) and 29.4 mg of  $\text{AgPF}_6$  (0.116 mmol) were dissolved in 3 mL of  $\text{CH}_2\text{Cl}_2$ , causing instant precipitation of metallic silver and  $[\text{4}](\text{PF}_6)_2$ . Due to a rather low stability of  $[\text{4}](\text{PF}_6)_2$ , attempts to isolate an analytically pure sample were not successful. Hence for the reaction with base we used a ca. 1:1 mol mixture of  $[\text{4}](\text{PF}_6)_2$  and Ag black obtained after decanting the green supernatant and drying the black-green powder *in vacuo*.

**Reaction of Radical Species  $1^{2+}$ ,  $2^{2+}$ , and  $4^{2+}$  with  $\text{K}_2\text{CO}_3$  (ref 56).** In a typical experiment 0.02 mmol of the metal complex  $1^{2+}$ ,  $2^{2+}$ , or  $4^{2+}$  (the isolated complexes were used in the case of  $1^{2+}$  and  $2^{2+}$ ; in the case of  $4^{2+}$  a mixture with co-precipitated metallic silver was used) was dissolved in 1 mL of acetone- $d_6$  and stirred with 0.4 mmol of anhydrous solid  $\text{K}_2\text{CO}_3$ . After the solution turned yellow, the recorded NMR spectra showed quantitative formation of  $1^+$ ,  $2^+$ , or  $4^+$ , respectively.

## ■ ASSOCIATED CONTENT

**Supporting Information.** Crystallographic information (cif file) containing data for complexes  $[\text{1}](\text{PF}_6)$ ,  $[\text{2}](\text{PF}_6)$ ,  $[\text{2}](\text{PF}_6)_2$ , and  $[\text{3}](\text{PF}_6)$ . The EPR spectra of  $4^{2+}$  and the reaction of  $1^{2+}$  with DMPO. This material is available free of charge via the Internet at <http://pubs.acs.org>.

## ■ AUTHOR INFORMATION

### Corresponding Author

\*Fax: (+31) 20 5255604. E-mail: b.debruin@uva.nl.

## ■ ACKNOWLEDGMENT

We thank Han Peeters for measuring the FAB $^+$ -MS mass spectrum. Financial support from the European Research Council (ERC Grant Agreement 202886-CatCIR), NWO-CW (VIDI grant 700.55.426), and the University of Amsterdam is gratefully acknowledged.

## ■ REFERENCES

- (1) Whittaker, J. W. *Chem. Rev.* **2003**, *103*, 2347–2363.
- (2) (a) Costas, M.; Mehn, M. P.; Jensen, M. P.; Que, L., Jr. *Chem. Rev.* **2004**, *104*, 939–986. (b) Limberg, C. *Angew. Chem., Int. Ed.* **2003**, *42*, 5932–5954.
- (3) Meunier, B.; de Visser, S. P.; Shaik, S. *Chem. Rev.* **2004**, *104*, 3947–3980.
- (4) Baik, M.-H.; Newcomb, M.; Friesner, R. A.; Lippard, S. J. *Chem. Rev.* **2003**, *103*, 2385–2419.
- (5) Stubbe, J.; Nocera, D. G.; Yee, C. S.; Chang, M. C. Y. *Chem. Rev.* **2003**, *103*, 2167–2201.
- (6) (a) Gridnev, A. A.; Ittel, S. D. *Chem. Rev.* **2001**, *101*, 3611–3659. (b) de Bruin, B.; Dzik, W. I.; Li, S.; Wayland, B. B. *Chem.—Eur. J.* **2009**, *15*, 4312–4320.
- (7) Penoni, A.; Wanke, R.; Tollari, S.; Gallo, E.; Musella, D.; Ragaini, F.; Demartin, F.; Cenini, S. *Eur. J. Inorg. Chem.* **2003**, 1452–1460.

- (8) (a) Sherry, A. E.; Wayland, B. B. *J. Am. Chem. Soc.* **1990**, *112*, 1259–1261. (b) Cui, W.; Zhang, X. P.; Wayland, B. B. *J. Am. Chem. Soc.* **2003**, *125*, 4994–4995. (c) Cui, W.; Wayland, B. B. *J. Am. Chem. Soc.* **2004**, *126*, 8266–8274. (d) Puschmann, F. F.; Grützmacher, H.; de Bruin, B. *J. Am. Chem. Soc.* **2010**, *132*, 73–75.
- (9) (a) Zhang, L.; Chan, K. S. *Organometallics* **2007**, *26*, 679–684. (b) Dzik, W. I.; Reek, J. N. H.; de Bruin, B. *Chem.—Eur. J.* **2008**, *14*, 7594–7599.
- (10) Königsmann, M.; Donati, N.; Stein, D.; Schönberg, H.; Harmer, J.; Sreekanth, A.; Grützmacher, H. *Angew. Chem., Int. Ed.* **2007**, *46*, 3567–3570.
- (11) Hetterscheid, D. G. H.; Klop, M.; Kicken, R. J. N. A. M.; Smits, J. M. M.; Reijerse, E. J.; de Bruin, B. *Chem.—Eur. J.* **2007**, *13*, 3386–3405.
- (12) For an overview see: Hicks, R. G. *Angew. Chem., Int. Ed.* **2008**, *47*, 7393–7395.
- (13) Copper: (a) Mankad, N. P.; Antholine, W. E.; Szilagy, R. K.; Peters, J. C. *J. Am. Chem. Soc.* **2009**, *131*, 3878–3880. Ruthenium: (b) Miyazato, Y.; Wada, T.; Muckerman, J. T.; Fujita, E.; Tanaka, K. *Angew. Chem., Int. Ed.* **2007**, *46*, 5728–5730. Nickel: (c) Adhikari, D.; Mossin, S.; Basuli, F.; Huffman, J. C.; Szilagy, R. K.; Meyer, K.; Mindiola, D. J. *J. Am. Chem. Soc.* **2008**, *130*, 3676–3682. For aminyl radicals coordinated to iridium and rhodium see ref 15.
- (14) (a) Roth, J. P.; Yoder, J. C.; Won, T.-J.; Mayer, J. M. *Science* **2001**, *294*, 2524–2526. (b) Yoder, J. C.; Roth, J. P.; Gussenhoven, E. M.; Larsen, A. S.; Mayer, J. M. *J. Am. Chem. Soc.* **2003**, *125*, 2629–2640. (c) Mader, E. A.; Larsen, A. S.; Mayer, J. M. *J. Am. Chem. Soc.* **2004**, *126*, 8066–8067. (d) Mader, E. A.; Davidson, E. R.; Mayer, J. M. *J. Am. Chem. Soc.* **2007**, *129*, 5153–5166. (e) Wu, A.; Mayer, J. M. *J. Am. Chem. Soc.* **2008**, *130*, 14745–14754. (f) Mader, E. A.; Manner, V. W.; Markle, T. F.; Wu, A.; Franz, J. A.; Mayer, J. M. *J. Am. Chem. Soc.* **2009**, *131*, 4335–4345.
- (15) (a) Büttner, T.; Geier, J.; Frison, G.; Harmer, J.; Calle, C.; Schweiger, A.; Schönberg, H.; Grützmacher, H. *Science* **2005**, *307*, 235–238. (b) Maire, P.; Königsmann, M.; Sreekanth, A.; Harmer, J.; Schweiger, A.; Grützmacher, H. *J. Am. Chem. Soc.* **2006**, *128*, 6578–6580. (c) Donati, N.; Stein, D.; Büttner, T.; Schönberg, H.; Harmer, J.; Anadaram, S.; Grützmacher, H. *Eur. J. Inorg. Chem.* **2008**, 4691–4703.
- (16) (a) Hetterscheid, D. G. H. Ph.D. Thesis, Radboud University Nijmegen, 2006. (b) Tejel, C.; Ciriano, M. A.; del Río, M. P.; van den Bruele, F. J.; Hetterscheid, D. G. H.; Tschlis i Spithas, N.; de Bruin, B. *J. Am. Chem. Soc.* **2008**, *130*, 5844–5845. (c) Tejel, C.; Ciriano, M. A.; del Río, M. P.; Hetterscheid, D. G. H.; Tschlis i Spithas, N.; Smits, J. M. M.; de Bruin, B. *Chem.—Eur. J.* **2008**, *14*, 10932–10936. (d) Tejel, C.; del Río, M. P.; Ciriano, M. A.; Reijerse, E. J.; Hartl, F.; Zális, S.; Hetterscheid, D. G. H.; Tschlis i Spithas, N.; de Bruin, B. *Chem.—Eur. J.* **2009**, *15*, 11878–11889.
- (17) Recently it was shown that replacement of cod ligand with dbcot greatly improved the (air) stability of an iridium catalyst for allylic substitutions: Spiess, S.; Welter, C.; Franck, G.; Taquet, J.-P.; Helmchen, G. *Angew. Chem., Int. Ed.* **2008**, *47*, 7652–7655.
- (18) (a) Fernandez, M. J.; Rodriguez, M. J.; Oro, L. A.; Lahoz, F. J. *J. Chem. Soc., Dalton Trans.* **1989**, 2073–2076. (b) Alvarado, Y.; Boutry, O.; Gutiérrez, E.; Monge, A.; Nicasio, M. C.; Poveda, M. L.; Pérez, P. J.; Ruiz, C.; Bianchini, C.; Carmona, E. *Chem.—Eur. J.* **1997**, *3*, 860–873.
- (19) Iimura, M.; Evans, D. R.; Flood, T. C. *Organometallics* **2003**, *22*, 5370–5373.
- (20) Dzik, W. I.; Smits, J. M. M.; Reek, J. N. H.; de Bruin, B. *Organometallics* **2009**, *28*, 1631–1643.
- (21) (a) Hermann, D.; Gandelman, M.; Rozenberg, H.; Shimon, L. J. W.; Milstein, D. *Organometallics* **2002**, *21*, 812–818. (b) Friedrich, A.; Ghosh, R.; Kolb, R.; Herdtweck, E.; Schneider, S. *Organometallics* **2009**, *28*, 708–718.
- (22) Shorter metal–ligand bond distances are generally interpreted to indicate stronger metal–ligand bond interactions. This however does not always reflect the actual thermodynamic metal–ligand bond dissociation (free) energies, which are also influenced by reorganization and solvation effects. See for instance: Huang, J.; Haar, C. M.; Nolan,



S. P.; Marshall, W. J.; Moloy, K. G. *J. Am. Chem. Soc.* **1998**, *120*, 7806–7815.

(23) Rossi, A. R.; Hoffmann, R. *Inorg. Chem.* **1975**, *14*, 365–374.

(24) Irngartinger, H.; Reibel, W. R. K. *Acta Crystallogr. B* **1981**, *B37*, 1724–1728.

(25) (a) [Rh(C<sub>6</sub>Cl<sub>5</sub>)<sub>2</sub>(cod)]: García, M. P.; Jiménez, M. V.; Oro, L. A.; Lahoz, F. J.; Casas, J. M.; Alonso, P. J. *Organometallics* **1993**, *12*, 3257–3263. (b) [Ir(C<sub>6</sub>Cl<sub>5</sub>)<sub>2</sub>(cod)]: García, M. P.; Jiménez, M. V.; Oro, L. A.; Lahoz, F. J.; Alonso, P. J. *Angew. Chem., Int. Ed.* **1992**, *31*, 1527–1529. (c) [( $\eta^5$ -C<sub>5</sub>Ph<sub>5</sub>)Rh(cod)]<sup>+</sup>: Shaw, M. J.; Geiger, W. E.; Hyde, J.; White, C. *Organometallics* **1998**, *17*, 5486–5491. (d) [Ir(Me<sub>3</sub>tpa)(C<sub>2</sub>H<sub>4</sub>)]<sup>2+</sup>: de Bruin, B.; Peters, T. P. J.; Thewissen, S.; Blok, A. N. J.; Wiltling, J. B. M.; de Gelder, R.; Smits, J. M. M.; Gal, A. W. *Angew. Chem. Int. Ed.* **2002**, *41*, 2135–2138. (e) For a review see: de Bruin, B.; Hetterscheid, D. G. H. *Eur. J. Inorg. Chem.* **2007**, 211–230.

(26) (a) Ogoshi, H.; Setsunu, J.; Yoshida, Z. *J. Am. Chem. Soc.* **1977**, *99*, 3869–3870. (b) Wayland, B. B.; Feng, Y.; Ba, S. *Organometallics* **1989**, *8*, 1438–1441.

(27) (a) Brammer, L.; Connelly, N. G.; Edwin, J.; Geiger, W. E.; Orpen, A. G.; Sheridan, J. B. *Organometallics* **1988**, *7*, 1259–1265. (b) Zhai, H.; Bunn, A.; Wayland, B. *Chem. Commun.* **2001**, 1294–1295. (c) Bunn, A. G.; Wayland, B. B. *J. Am. Chem. Soc.* **1992**, *114*, 6917–6919.

(28) Both compounds could be oxidized by Ag<sup>+</sup> in acetone. 2<sup>+</sup> was prepared by oxidation with [Fe( $\eta^5$ -C<sub>5</sub>H<sub>4</sub>COMe)Cp]<sup>+</sup> in CH<sub>2</sub>Cl<sub>2</sub>; however this oxidant was too weak to oxidize 1<sup>+</sup>. For a list of common redox agents in organometallic chemistry see: Connelly, N. G.; Geiger, W. E. *Chem. Rev.* **1996**, *96*, 877–910.

(29) (a) Hetterscheid, D. G. H.; Grützmacher, H.; Koekoek, A. J. J.; de Bruin, B. *Prog. Inorg. Chem.* **2007**, *55*, 247–354. (b) Wassenaar, J.; de Bruin, B.; Siegler, M. A.; Spek, A. L.; Reek, J. N. H.; van der Vlugt, J. I. *Chem. Commun.* **2010**, 47, 1232–1234. For examples of related [Rh(N<sub>3</sub>-ligand)(diolefin)]<sup>+2+</sup> complexes see also ref 11 and (c) Hetterscheid, D. G. H.; Smits, J. M. M.; de Bruin, B. *Organometallics* **2004**, *23*, 4236–4246.

(30) (a) Hetterscheid, D. G. H.; Kaiser, J.; Reijerse, E. J.; Peters, T. P. J.; Thewissen, S.; Blok, A. N. J.; Smits, J. M. M.; de Gelder, R.; de Bruin, B. *J. Am. Chem. Soc.* **2005**, *127*, 1895–1905.

(31) In acetone-d<sub>6</sub> a very slow rise of the signals of the diamagnetic precursor could be observed for both complexes, in the case of the rhodium complex 1<sup>2+</sup> accompanied by the rise of signals of the free dbcot moiety. Kinetic measurements using UV/vis spectrometry revealed that the decomposition of 1<sup>2+</sup> and 2<sup>2+</sup> proceeds according to a first-order rate equation in the metal complex concentration with  $k_{\text{obs}} = 1 \times 10^{-6}$  and  $4 \times 10^{-7} \text{ s}^{-1}$ , respectively. Addition of H<sub>2</sub>O increases the rate of decomposition considerably, however, in the case of 1<sup>2+</sup> in an aselective manner.

(32) The same results were obtained when exactly 1 equiv of KO<sup>t</sup>Bu was added. This base however proved to be less suitable, because if used in excess, some follow-up unselective reactivity was observed. Indeed, treatment of the iridium(I) compound 2<sup>+</sup> with 1 equiv of KO<sup>t</sup>Bu in THF produces a red precipitate (insoluble in all common organic solvents) and the free bla ligand. This is most likely due to double bla ligand deprotonation (see also ref 16), as double bpa ligand deprotonation reactions of related [(bpa)M(cod)]<sup>+</sup> (M = Rh, Ir) complexes has been observed in our group. This will be described in a separate paper.

(33) If the aminyl radical would abstract a hydrogen atom from the solvent, one would expect that mostly deuterium would be incorporated. Alternatively a very large kinetic isotope effect could explain the obtained hydrogen atom; see: Huynh, M. H. V.; Meyer, T. J. *Proc. Natl. Acad. Sci. U. S. A.* **2004**, *101*, 13138–13141.

(34) Evans, C. A. *Aldrichim. Acta* **1979**, *12*, 23–29.

(35) Radical trapping of species 1<sup>2+</sup> in acetone solution using DMPO (DMPO = 5,5-dimethyl-1-pyrroline-N-oxide) revealed formation of at least two species, A and B; however neither of these could be assigned to a solvent radical and most probably a rhodium radical has

been captured. These species existed in a 1:0.1 ratio, which changed in time. Simulated parameters: I (major):  $g_{\text{iso}} = 2.007$ ,  $A^{\text{N}} = 48.9 \text{ MHz}$ ,  $A^{\text{H}} = 56.6 \text{ MHz}$ ,  $A^{\text{Rh}} = 4.9 \text{ MHz}$ ; II (minor):  $g_{\text{iso}} = 2.0049$ ,  $A^{\text{N}} = 46.3 \text{ MHz}$ ,  $A^{\text{H}} = 57.5 \text{ MHz}$ . See Supporting Information. Species 2<sup>2+</sup> with DMPO and K<sub>2</sub>CO<sub>3</sub> gave a complex, very low intensity signal, which was impossible to simulate reliably.

(36) The oxidation of CO<sub>3</sub><sup>2-</sup> to C<sub>2</sub>O<sub>6</sub><sup>2-</sup> seems to be less probable. Although the redox potential of the C<sub>2</sub>O<sub>6</sub><sup>2-</sup>/CO<sub>3</sub><sup>2-</sup> couple in aqueous carbonate buffer is +0.67 V vs Fc/Fc<sup>+</sup> (0.21 vs SCE), the low concentration of carbonate anions in acetone makes this pathway energetically unfavorable. Zhang, J.; Oloman, C. W. *J. Appl. Electrochem.* **2005**, *35*, 945–953.

(37) As suggested by a referee, reaction in dry dmsO (which is not susceptible to deprotonation) could give more mechanistic information. Hence, we investigated the reactivity of radical compound 4<sup>2+</sup> in dmsO. Unfortunately, however, the radical complex proved highly unstable in dry dmsO-d<sub>6</sub> (<1 mol % H<sub>2</sub>O per Rh), in which it immediately decomposes to form a mixture of diamagnetic compounds even in the absence of a base. Complex 4<sup>2+</sup> is stable for much longer in pure acetone. The reaction in dmsO-d<sub>6</sub> does produce significant amounts of the rhodium(I) compound 4<sup>+</sup>, but in this solvent the reaction is not clean and substantial amounts of other unidentified products and free dbcot were observed (perhaps indicating a redox disproportionation reaction). Hence, the results in dmsO are mechanistically inconclusive for the reactions in acetone.

(38) This equilibrium lies on the side of 1<sup>2+</sup>/2<sup>2+</sup> and acetone (the oxidation of acetone occurs over 1000 mV vs the Fc/Fc<sup>+</sup> couple,<sup>11</sup> which gives an energy difference between the two sides of the equilibrium of roughly 600–700 mV or 14–16 kcal/mol).

(39) The redox potential of the <sup>•</sup>OH/<sup>•</sup>OH couple in MeCN is only +0.29 vs Fc/Fc<sup>+</sup> (+0.96 vs NHE): (a) Sawyer, D. T.; Roberts, J. K., Jr. *Acc. Chem. Res.* **1988**, *21*, 469–476. (b) Calculated from the relationship  $\text{NHE} - E_{1/2} \text{ Fc/Fc}^+ = 630 \text{ mV}$ : Pavlishchuk, V. V.; Addison, A. W. *Inorg. Chim. Acta* **2000**, *298*, 97–102.

(40) (a) Ortep-3 for Windows: Farrugia, L. J. *J. Appl. Crystallogr.* **1997**, *30*, S65. (b) Rendering was made with POV-Ray 3.6. *Persistence of Vision Raytracer* (Version 3.6), Persistence of Vision Pty. Ltd., 2004. Retrieved from <http://www.povray.org/download/>.

(41) Treutler, O.; Ahlrichs, R. *J. Chem. Phys.* **1995**, *102*, 346–354.

(42) PQS version 2.4; Parallel Quantum Solutions: Fayetteville, AR, USA, 2001. The Baker optimizer is available separately from PQS upon request. Baker, J. J. *Comput. Chem.* **1986**, *7*, 385–395.

(43) Sierka, M.; Hoge Kamp, A.; Ahlrichs, R. *J. Chem. Phys.* **2003**, *118*, 9136–9148.

(44) (a) Becke, A. D. *Phys. Rev. A* **1988**, *38*, 3098–3100. (b) Perdew, J. P. *Phys. Rev. B* **1986**, *33*, 8822–8824.

(45) Schaefer, A.; Horn, H.; Ahlrichs, R. *J. Chem. Phys.* **1992**, *97*, 2571–2577.

(46) (a) g-tensor: van Lenthe, E.; van der Avoird, A.; Wormer, P. E. S. *J. Chem. Phys.* **1997**, *107*, 2488. (b) A-tensor: van Lenthe, E.; van der Avoird, A.; Wormer, P. E. S. *J. Chem. Phys.* **1998**, *108*, 4783.

(47) te Velde, G.; Bickelhaupt, F. M.; van Gisbergen, S. J. A.; Fonseca Guerra, C.; Baerends, E. J.; Snijders, J. G.; Ziegler, T. *J. Comput. Chem.* **2001**, *22*, 931.

(48) (a) Lee, C.; Yang, W.; Parr, R. G. *Phys. Rev. B* **1988**, *37*, 785–789. (b) Becke, A. D. *J. Chem. Phys.* **1993**, *98*, 1372–1377. (c) Becke, A. D. *J. Chem. Phys.* **1993**, *98*, 5648–5652.

(49) Eichkorn, K.; Weigend, F.; Treutler, O.; Ahlrichs, R. *Theor. Chem. Acc.* **1997**, *97*, 119–124.

(50) (a) Anton, D. R.; Crabtree, R. H. *Organometallics* **1983**, *2*, 621–627. (b) Singh, A.; Sharp, P. R. *Inorg. Chim. Acta* **2008**, *361*, 3159–3164.

(51) van der Ent, A.; Onderdenlinden, A. L. *Inorg. Synth.* **1990**, *28*, 90–91.

(52) Chaffins, S.; Brettreich, M.; Wudl, F. *Synthesis* **2002**, *9*, 1191–1194. Instead of Li sand (as described in the original procedure), for performing the first step we used granular Li (0.5% Na) and obtained dbcot in 15% overall yield.

(53) de Bruin, B.; Brands, J. A.; Donners, J. J. J. M.; Donners, M. P. J.; de Gelder, R.; Smits, J. M. M.; Gal, A. W.; Spek, A. L. *Chem.—Eur. J.* **1999**, *5*, 2921–2936.

(54) Komatsu, K.; Kikuchi, K.; Kojima, H.; Urano, Y.; Nagano, T. *J. Am. Chem. Soc.* **2005**, *127*, 10197–10204.

(55) Bain, G. A.; Berry, J. F. *J. Chem. Educ.* **2008**, *85*, 532–536.

(56) The radical complexes  $[1](PF_6)_2$ ,  $[2](PF_6)_2$ , and  $[4](PF_6)_2$  are all well soluble in acetone and acetonitrile. In contrast to  $[1](PF_6)_2$  and  $[2](PF_6)_2$ , complex  $[4](PF_6)_2$  is also slightly soluble in  $CH_2Cl_2$ .

#### ■ NOTE ADDED AFTER ASAP PUBLICATION

This paper was published ASAP on March 10, 2011. An entry in Table 1 was updated. The revised paper was reposted on March 16, 2011.